

Analysis of the Wire/Substrate Interface during Ultrasonic Bonding Process

Yangyang Long^{1)*}, Folke Dencker²⁾, Andreas Isaak²⁾,
Chun Li¹⁾, Marc Wurz²⁾, Jens Twiefel¹⁾, Jörg
Wallaschek¹⁾

¹⁾Institute of Dynamics and Vibration Research

²⁾Institute of Micro Production Technology

Leibniz Universität Hannover

Hanover, Germany

*long@ids.uni-hannover.de

Friedrich Schneider, Jörg Hermsdorf
Materials & Processes Department
Laser Zentrum Hannover, e.V.
Hanover, Germany

Abstract—The ultrasonic wire bonding has been applied in the semiconductor packaging industry ever since its innovation in the 1960s. The mechanisms of the bonding process, however, are still unclear. According to state-of-the-art, the extremely short bonding process can be divided into four phases. These phases at the bonding interface were analyzed either from a side view or from a 2-D view but only after the bonding process when the wire was removed or cut. A 2-D real-time observation at the bonding interface, which is beneficial to a deeper understanding on these phases, has not been conducted. In this work, a transparent glass was used as the substrate and a high-speed observation system was installed underneath the glass to real-time observe the different phases from a 2-D view. The wire/substrate contact area and the friction area as well as their expansion over time were first observed. During this period, the oxide scale breakage area can be detected. A static dark area related to the formation of microwelds then appeared from the central region. During the expansion of this area, some oxides retained within this static area while most oxides were carried to the peripheral contact area. Friction continued during the extension of the contact area and the static area. These findings provide a deeper insight into the wire bonding process.

Keywords—ultrasonic wire bonding; wire/substrate interface; real-time observation

I. INTRODUCTION

The bondability of metals by ultrasound (US) was discovered by accident in the late 1940s while after ~10 years the ultrasonic wire bonding technology was introduced to the semiconductor packaging industry [1]. In spite of the wide application of this technique, the bonding mechanisms still lack a complete understanding, especially from a quantitative point of view. This is due to the complicated change of the physical phenomena occurring during the ultra-short process time. Four phases [1] can be used to describe the bonding process and the phenomena: 1) Pre-deformation and activation of US vibration, 2) Friction, 3) US softening and 4) Interdiffusion. During phase 1), a normal force is loaded leading to a geometry change of the wire and a contact change from line contact to area contact [2]. Since the vibration amplitude of the tool is too small during the activation stage of

US vibration, no relative motion between the wire and the substrate occurs [3]. The friction at the wire/substrate interface has been extensively studied, but only from a side view and the friction route at different contact areas were considered to be similar [4-6]. During the softening phase, macroscopic plastic deformation continues and microwelds are formed. The plastic deformation has been in-situ measured [7] while the microwelds have been hardly studied [8]. The formation of the microwelds area as well as its expansion was only observed when the wire was removed after the bonding process [9] or indirectly measured [10]. Once a microweld forms, interdiffusion immediately starts. The interdiffusion first locally takes place at different locations and then extends to the whole interface [11]. The first three phases are the focus of this work.

In this work, the two-dimensional wire/substrate interface is real-time observed by using a high-speed observation system through a transparent glass substrate. All the phenomena except interdiffusion can be observed and quantified. Even though metal-glass bonding is different from metal-metal bonding, the processes are assumed to be similar. Therefore the knowledge gained for the metal-glass bonding leads to a better understanding on the mechanisms behind.

II. EXPERIMENTAL SETUP

A. Bonding setup

The Al-H11 aluminum wire with a diameter of 400 μm was purchased from Heraeus GmbH and used in this work. The breaking load of the wire is 500~700 cN with more than 5% elongation. The thick aluminum wire bonding head HBK05 is provided by Hesse Mechatronics GmbH. The natural frequency of the transducer in the bonding head is around 60 kHz and is driven by an in-house developed digital phase controller [12] and a Brüel & Kjær 2713 amplifier. The substrate used is a transparent silicon dioxide glass with a dimension of 40 x 40 x 3 mm and a surface roughness of less than 1.2 nm from Siegert Wafer GmbH. The focal plane is the wire/glass interface and the observation direction is shown in Fig. 1.

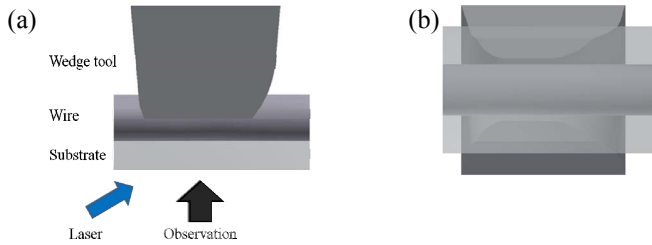


Fig. 1 Observation position (a) side view (b) bottom view

B. High-speed observation system

A high-speed observation system is used for real-time observation. It consists of a high-speed camera Phantom v710 from Vision Research Inc. and an 18X magnification system. The whole system has a resolution of 1.1 $\mu\text{m}/\text{pixel}$ and applied a record rate of 20,000 fps with a window size of 640 x 480 pixel. A laser source JOLD-45-CPXF-1P from Jenoptic AG was used for illumination. The illumination light injected from bottom with a large angle to the observation system. The light was then reflected by the wire/glass interface and then collected by the observation system.

III. RESULTS AND DISCUSSION

A. A typical process

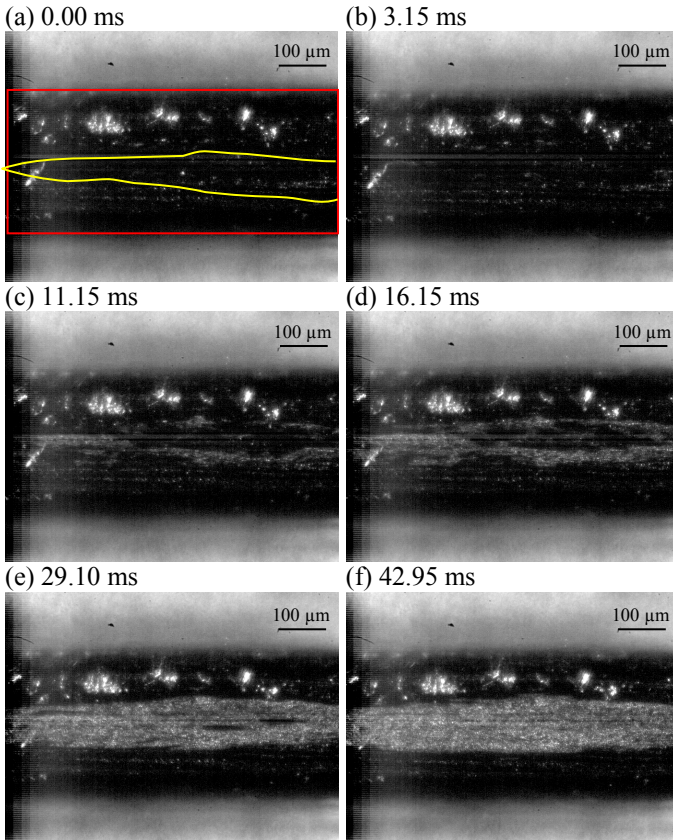


Fig. 2 Friction induced oxide scale breakage

The metal-glass bonding process was undertaken with a normal force of 5 N, an US power of 1.3 W and the process lasted for 400 ms. Three different areas, contact area, friction

area and static area, can be observed in the recorded video and are explained in details as the following.

After the loading of the normal force, the wire/glass contact switched from a line contact to an elliptic contact. As shown in Fig. 2 (a), the red rectangular shows the wire and the contact boundary is marked by the yellow curve. At this moment, the interface showed a low brightness due to the weak light reflection of the flat wire surface. As US vibration was activated, the top layer of the wire surface which is the natural oxide layer started to get broken. The oxide scale was first detached from the pure metal surface and then rolled into small particles. The oxide particles can effectively reflect the illumination light as they possess many facets with different angles. Since the vibration of the wire at the peripheral region was more serious, only the peripheral region of the contact showed a high brightness in the beginning, as shown in Fig. 2 (b)(c)(d). As vibration continued, the oxides in the central region got broken and finally the whole contact area was covered by oxide particles at ~29.10 ms (see Fig. 2 (e)(f)).

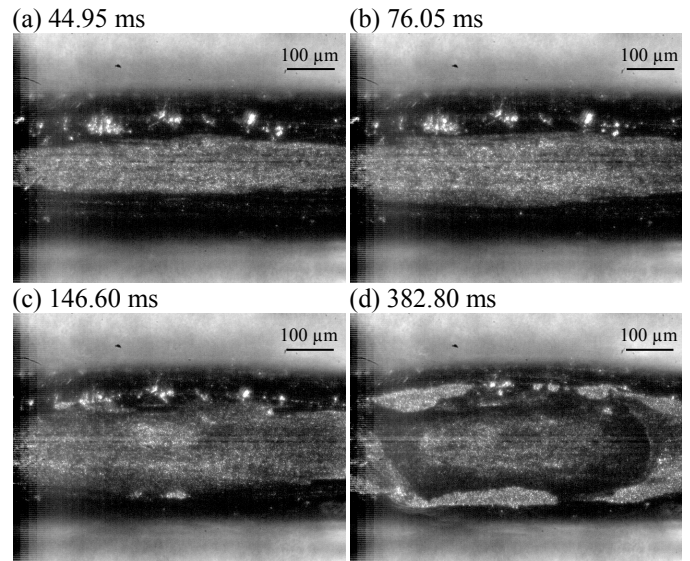


Fig. 3 Expansion of contact area

In the meantime of the friction, some US energy was transferred from the tool tip to the wire and got absorbed by the defects inside the crystals of the wire. The defects, especially the dislocations, were pushed away from their pinned position, which led to a lower yield stress of the wire material. Together with the stress superposition, continuous plastic deformation and its induced material flow at the wire/tool interface took place. As shown in Fig. 3, the contact area as well as the friction area got enlarged until the end of the bonding process.

At ~152.85 ms during the expansion of the contact area, another dark layer appeared as marked in Fig. 4 (a). Different from the other part of the wire, this dark area kept static. The vibration amplitude of the surrounding area became smaller and smaller until the dark layer covered this area which became static as well. As can be seen in Fig. 4, this dark layer expanded until the bonding process terminated. During the extension of the static area, some oxide particles retain inside

the static area as indicated by their brightness. The extension rate of the static area from Fig. 4 (c) to (d) is faster than the other moments and large amount of oxides left within this expansion period. The moving of this oxide region was stopped by the microwelds formation surrounding the area. Outside of the central bright area, as shown in Fig. 4 (e) and (f), the brightness became low again, which indicates a high removal rate of oxides at these areas.

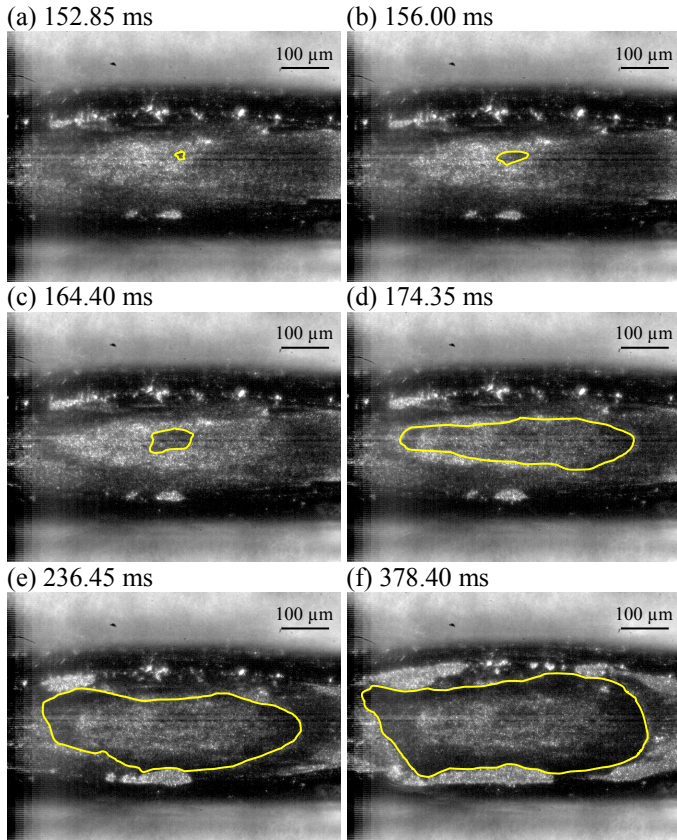


Fig. 4 Expansion of the microwelds-oxides mixture area

As a result, three different areas which are contact area, friction area and static area appeared in the recorded process. The contact area first appeared during the loading of the normal force and continually increased during the bonding process. The friction area can be then observed when the oxide scale got detached and broken after a couple of vibration cycles. It extended outwards due to the continuous vibration and the expansion of the contact area. After certain time, a static area emerged due to the formation of microwelds. During the expansion of the static area, more microwelds were formed while some oxides retained. In other words, the static area is a mixture of microwelds and oxides. The microwelds and oxides can be identified by their brightness. Since the relative motion at the central region was comparably small, only little oxides can be carried out. Most oxides were transported to the peripheral region outside of the static region and showed a very high brightness. The best bonded region was between the inner oxide region and the peripheral region under the applied parameters. This result supported the assumption in [13].

B. Quantification of four areas

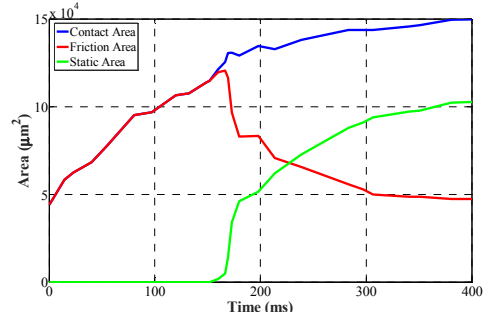


Fig. 5 Quantification of the four areas during the bonding process

As can be seen from Fig. 5, the contact area and the friction area extended fast in the beginning stage and the extension became slower and slower. Due to the appearance of the static area, the friction area significantly shrank. The static area grew slow after its emergence and then increased fast. As the increase of the contact area got slow, the growth of the static area became slow as well since the peripheral region cannot be bonded due to the strong relative motion. Along with the static area expansion, more microwelds area formed.

C. End region

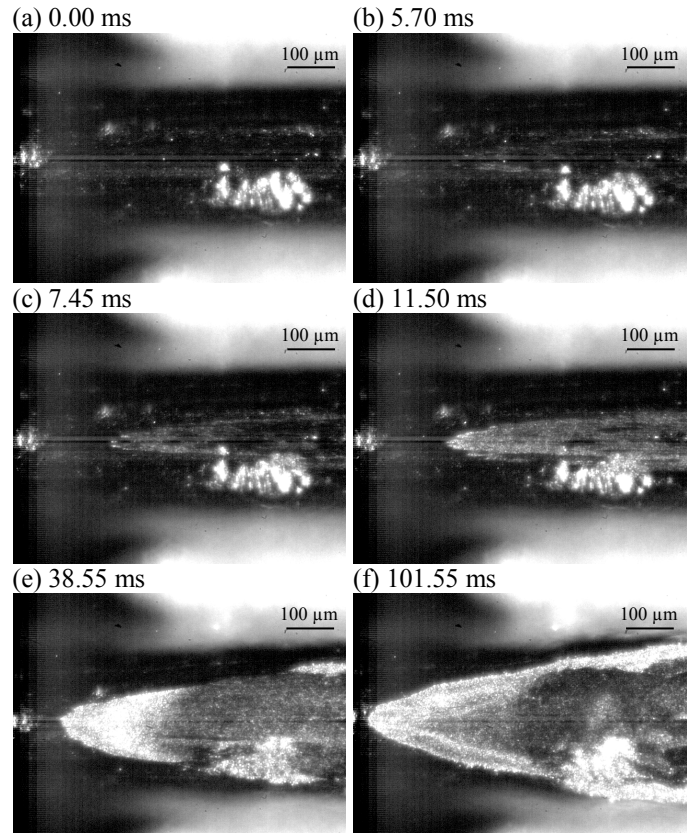


Fig. 6 Expansion of contact and friction area

Due to the small window size and the long dimension of the contact, the whole wire/glass interface was unable to be recorded in one video with high frame rate. Therefore, the record window was moved to the end region of the contact for

recording the different areas within this region. As shown in Fig. 6, the friction was more serious at the peripheral region and led to the breakage of the oxide scale. Simultaneously, the contact area expanded due to the US vibration induced acoustoplasic effect. The expansion of the contact area at the wire direction can be clearly observed in Fig. 6 (d) to (f). As mentioned above, a static area appeared after a certain time. However, this area does not have to start from the central region. For this specimen, the static area emerged at a corner of the contact shown in Fig. 7 (a). It locally expanded and finally connected with the static area that started in the central region of the contact, as can be seen in Fig. 7 (d). The same as the static region in the central contact area, some oxides retained inside the static area and prohibited the microwelds formation at these locations.

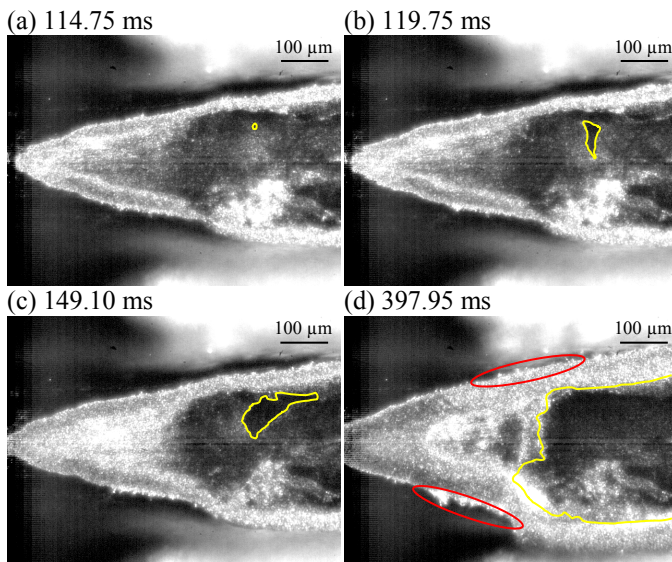


Fig. 7 Expansion of static area

Another thing that can be observed is the oxide particles which were compelled to the outside of the contact. As in the red ellipses of Fig. 7 (d), these oxide particles appeared when the continuous plastic deformation vanished. In other words, the vibration induced relative motion between the wire and the substrate caused this.

When the contact end region did not fulfill the recording window, the vibration of the wire outside of the contact can be observed. After the appearance of the static area, different parts of the wire showed different vibration amplitudes due to the low stiffness of the wire material. On the other hand, the vibration amplitude of the wire only decreases, but never reach zero when it is observed from a side view.

IV. CONCLUSION

In this work, the real-time observation of the bonding process at the wire/substrate interface provides a deeper insight on the mechanisms. In both the middle region and the end region of the contact, three different areas including contact area, friction area and static area as well as their changes were detected and quantified. The quantification of

these areas shows the fast growth of the contact area and the friction area in the beginning stage and a slow growth trend in the latter stage. The friction caused the breakage of oxide scale, which started from the peripheral contact region. For the first time, the static area consisting of microwelds and oxides was observed. Most oxides were carried to the peripheral region of the contact while some retained within the static area. US vibration induced relative motion helped the transportation of oxides.

Acknowledgment

This work is supported by DFG (Deutsche Forschungsgemeinschaft) programm (TW75/8-1|WA564/40-1|WU 558/11-1). Many thanks to Hesse Mechatronics GmbH for providing the bonding head HBK05.

References

- [1] Y. Long, J. Twiefel and J. Wallaschek, "A review on the mechanisms of ultrasonic wedge-wedge bonding," *J. Mater. Process. Technol.*, vol. 245, pp. 241-258, July 2017.
- [2] Osterwald, F., Verbindungsbildung beim ultraschall-Drahtbonden: Einfluß der Schwingungsparameter und Modellvorstellungen, Technical University of Berlin, 1999.
- [3] H. Gaul, M. Schneider-Ramelow, K. D. Lang and H. Reichl, "Predicting the shear strength of a wire bond using laser vibration measurements," in *IEEE Electron. Syst.-Integ. Technol. Conf.*, 2006, pp. 719-725.
- [4] H. Gaul, M. Schneider-Ramelow and H. Reichl, "Analysis of the friction processes in ultrasonic wedge/wedge-bonding," *Microsys. Technol.*, vol. 15, pp. 771-775, May 2009.
- [5] H. Gaul, A. Shah, M. Mayer, Y. Zhou, M. Schneider-Ramelow and H. Reichl, "The ultrasonic wedge/wedge bonding process investigated using in situ real-time amplitudes from laser vibrometer and integrated force sensor," *Microelectron. Eng.*, vol. 87, pp. 537-542, April 2010.
- [6] A. Unger, W. Sextro, T. Meyer, P. Eichwald, S. Althoff, F. Eacock, M. Brökelmann, M. Hunstig and K. Guth, "Modeling of the stick-slip effect in heavy copper wire bonding to determine and reduce tool wear," in *Electron. Pack. Technol. Conf.*, 2015., pp. 1-4.
- [7] U. Geißler, M. Schneider-Ramelow and H. Reichl, "Hardening and softening in AlSi1 bond contacts during ultrasonic wire bonding," *IEEE Trans. Compon. Packag. Technol.*, vol. 32, pp. 794-799, December 2009.
- [8] M. Maeda, K. Yamane, S. Matsusaka and Y., Takahashi, "Relation between vibration of wedge-Tool and adhesion of wire to substrate during ultrasonic bonding," *Q. J. Japan Weld. Soc.*, vol. 27, pp. 200-203, August 2009.
- [9] Y. Zhou, X. Li and N.J. Noolu, "A footprint study of bond initiation in gold wire crescent bonding," *IEEE Trans. Compon. Packag. Technol.*, vol. 28, pp. 810-816, December 2005.
- [10] H., Seppänen, R., Kurppa, A., Meriläinen and E., Häggström, "Real time contact resistance measurement to determine when microwelds start to form during ultrasonic wire bonding," *Microelectron Eng.*, vol. 104, pp. 114-119, April 2013
- [11] U. Geissler, J. Funck, M. Schneider-Ramelow, H.-J. Engelmann, I. Rooch, W.H. Müller and H. Reichl, "Interface formation in the US-wedge/wedge-bondprocess of AlSi1/CuNiAu contacts," *J. Electron. Mater.*, vol. 40, pp. 239-246, February 2011
- [12] I. Ille and J. Twiefel, "Model-Based Feedback Control of an Ultrasonic Transducer for Ultrasonic Assisted Turning Using a Novel Digital Controller," *Phys. Procedia*, vol. 70, pp. 63-67, 2015.
- [13] V.H.I. Winchell and H. Berg, "Enhancing ultrasonic bond development," *IEEE Trans. Compon., Hybrids, Manuf. Technol.*, vol. 1, pp. 211-219, September 1978.